Antidepressants bind to cholesterol-interaction motif of TRKB neurotrophin receptor

Authors:
Plinio C Casarotto[1], Mykhailo Girych[2], Senem M Fred[1], Rafael Moliner[1], Giray Enkavi[2], Caroline Biojone[1], Cecilia Cannarozzo[1], Cecilia A Brunello[1], Anna Steinzeig[1], Frederike Winkel[1], Sudarshan Patil[3], Stefan Vestring[4], Tsvetan Serchov[5], Vera Kovaleva[6], Cassiano RAF Diniz[1,7], Liina Laukkanen[1], Iseline Cardon[8], Hanna Antila[1,9], Tomasz Rog[2], Mart Saarma[6], Clive R Bramham[3], Claus Normann[4], Sari E Lauri[1,10], Ilpo Vattulainen[2,11], Eero Castrén[1]*

1. Neuroscience Center - HILIFE, University of Helsinki, Finland.
2. Department of Physics, University of Helsinki, Finland.
3. Department of Biomedicine and KG Jebsen Center for Research on Neuropsychiatric Disorders, University of Bergen, Norway.
4. Center for Neuromodulation, Department of Psychiatry and Psychotherapy, Medical Center, Faculty of Medicine, University of Freiburg, Germany.
5. Department of Stereotactic and Functional Neurosurgery, Laboratory of Stereotaxy and Interventional Neuroscience, Medical Center – University of Freiburg, Faculty of Medicine, University of Freiburg, Germany.
6. Institute of Biotechnology - HILIFE, University of Helsinki, Finland.
7. Department of Pharmacology. Ribeirão Preto Medical School. University of São Paulo, Brazil.
8. Brain Master Program, Faculty of Science, Aix-Marseille Université, Marseille, France.
9. Department of Neuroscience, Perelman School of Medicine, University of Pennsylvania, PA, USA.
10. Molecular and Integrative Biosciences Research Program, University of Helsinki, Finland.
11. Computational Physics Laboratory, Tampere University, Finland.

* Lead contact:
Eero Castren. eero.castren@helsinki.fi

Abstract

It is unclear how binding of antidepressant drugs to their targets gives rise to the clinical antidepressant effect. We discovered that the transmembrane domain of TRKB, a BDNF receptor promoting neuronal plasticity and antidepressant responses, has a cholesterol-interaction site that may mediate the synaptic effects of cholesterol. We then found that both typical and fast-acting antidepressants bind to this cholesterol-interaction motif, thereby facilitating synaptic localization of TRKB and its activation by BDNF. Docking simulations revealed a binding site at the transmembrane region of TRKB dimers. Mutation of the TRKB cholesterol-interaction motif or cholesterol depletion impaired BDNF-mediated plasticity, as well as cellular and behavioral responses to antidepressants *in vitro* and *in vivo*. We suggest that binding to TRKB and the allosteric facilitation of BDNF signaling is the common mechanism for antidepressant action, which proposes a framework for how molecular effects of antidepressants are translated into clinical mood recovery.

Introduction

Several targets for antidepressant drug action have been identified but it is not clear how binding to these targets is translated into the clinical effects. Classical antidepressants, such as tricyclic antidepressants and serotonin selective reuptake inhibitors (SSRI), increase the synaptic levels of serotonin and noradrenaline by inhibiting reuptake or metabolism, but it has been unclear why their clinical effects appear with a substantial delay, while the effects on monoamines take place fast (Abdallah et al., 2015; Belmaker and Agam, 2008). The recently described rapid antidepressant effect of ketamine is attributed to inhibition of NMDA-type glutamate receptors (Abdallah et al., 2015; Belmaker and Agam, 2008; Berman et al., 2000; Zarate et al., 2006). However, 2R,6R-hydroxynorketamine (R,R-HNK), a ketamine metabolite with antidepressant-like activity, was found to exhibit low affinity to NMDA receptors, which has called the role of NMDA receptors in the ketamine action into question (Zanos et al., 2016, 2018). Therefore, it is not clear whether there is a common mechanism behind the antidepressant effect.

Essentially all antidepressants, including ketamine and R,R-HNK, increase the expression of brain-derived neurotrophic factor (BDNF) and activate BDNF signaling through Neurotrophic Tyrosine Kinase Receptor 2 (TRKB) (Autry and Monteggia, 2012; Castrén and Antila, 2017; Duman and Monteggia, 2006). These effects of SSRIs and ketamine on neurotrophin signaling have been considered to be indirect, through the inhibition of serotonin transporter (5HTT) and NMDA receptors, respectively. BDNF mimics the effects of antidepressants in rodents while inhibiting TRKB signaling prevents their behavioral effects (Autry and Monteggia, 2012; Castrén and Antila, 2017; Duman and Monteggia, 2006; Saarelainen et al., 2003). Activation of TRKB is a critical mediator of activity-dependent synaptic plasticity (Park and Poo, 2013) and the antidepressant-induced BDNF-TRKB signaling reactivates a juvenile-like state of plasticity in the adult brain, which has been suggested to underlie the effects of antidepressant treatments on mood (Castrén and Antila, 2017; Karpova et al., 2011; Maya Vetencourt et al., 2008).

The activation of TRKB by BDNF is bidirectionally linked to brain cholesterol metabolism. BDNF promotes production of cholesterol in neurons (Suzuki et al., 2007; Zonta and Minichiello, 2013) and cholesterol regulates TRKB signaling (Pereira and Chao, 2007; Suzuki et al., 2004). Cholesterol is essential for neuronal maturation and proper synaptic transmission (Martin et al., 2014; Mauch et al., 2001). Cholesterol is assumed not to pass the blood-brain barrier, therefore, neurons are dependent on locally synthesized cholesterol. Astrocytes are the main source of brain cholesterol that is then transported to neurons through an ApoE-mediated mechanism (Pfrieger and Ungerer, 2011). Synaptic cholesterol levels are low during the embryonic and early postnatal life but strongly increase during the 3rd postnatal week in mice (Suzuki et al., 2004)(Tulodziecka et al., 2016). Such increase in synaptic cholesterol levels coincides with the increase in BDNF expression and appearance of antidepressants effects on TRKB (Castrén and Antila, 2017; Di Lieto et al., 2012). Many antidepressants interact with phospholipids and accumulate in cholesterol-rich membrane microdomains, such as lipid rafts (Erb et al., 2016; Wray et al., 2018).

This data prompted us to investigate the potential interactions between TRKB, cholesterol and antidepressants. We found a putative cholesterol interaction motif within the TRKB transmembrane (TM) region, suggesting that interaction with TRKB and promotion of its signaling mediates at least part of the plasticity-promoting effects of neuronal cholesterol. Furthermore, we found that different antidepressant drugs directly bind to a site formed by a dimer of these cholesterol interaction sites within the TRKB TM domain, thereby facilitating cell surface expression of TRKB and promoting BDNF signaling. These data suggest that direct binding to TRKB and promotion of BDNF-mediated plasticity is a novel mechanism of action for antidepressant drugs.

Results

CARC motif regulates TRKB activation

Cholesterol is known to promote neuronal maturation and plasticity, but the mechanisms through which cholesterol exerts these effects have remained unclear (Martin et al., 2014; Mauch et al., 2001; Pfrieger and Ungerer, 2011). It has been proposed that steroids interact with proteins by binding to domains called Cholesterol-Recognition and Alignment Consensus (CRAC) or its inverted version CARC (Fantini et al., 2019). We conducted a bioinformatic mining of TRK receptors using the algorithm for CRAC and CARC. The results revealed a motif in the TRKB transmembrane (TM) region that fulfils the criteria for CARC. This motif is specific to TRKB and is not present in other TRK receptors (Fig. S1A), and it suggests that cholesterol might directly interact with TRKB. Indeed, cholesterol added to the culture media at 20μM enhanced the effects of BDNF (10ng/ml) on TRKB phosphorylation (pTRKB) in primary cortical neurons. However, at higher concentrations (50-100μM), cholesterol suppressed the effects of BDNF (Fig. 1A). Cholesterol promoted the interaction of TRKB with phospholipase C-gamma1 (PLC-γ1), a critical mediator of TRKB intracellular signaling (Minichiello et al., 2002) (Fig. 1B, S1C). The majority of TRKB resides in intracellular vesicles not accessible to BDNF (Du et al., 2000; Haapasalo et al., 2002; Meyer-Franke et al., 1998). We found that cholesterol treatment increased the translocation of TRKB to the cell surface in fibroblasts expressing TRKB, but not in cells expressing TRKA (Fig. S1D,F). The effects of BDNF on TRKB-PLC-γ1 interaction (Fig. 1B), as well as on neurite branching in cultured cortical neurons (Fig. S1H-L) were prevented by prior treatment with pravastatin (1μM/3d), an inhibitor of cholesterol synthesis, as reported previously (Suzuki et al., 2004). A higher concentration of pravastatin (2μM/5d) reduced the survival of cultured cortical neurons and this effect was attenuated by exogenous cholesterol (20μM), but not by BDNF (Fig. S1M,N), indicating that the effects of pravastatin are mediated through inhibition of cholesterol synthesis.

Tyrosine residue in the center of CARC motif is predicted to be critical for cholesterol interaction (Fantini and Barrantes, 2013). Mutation of the critical tyrosine 433 in the TRKB CARC motif into phenylalanine (TRKB.Y433F) did not influence the binding affinity of BDNF (TRKB.wt=0.081ng/ml;

TRKB.Y433F=0.076ng/ml; Fig. S1O). However, this mutation reduced the BDNF-induced increase in the phosphorylation of TRKB (pTRKB) at the PLC-γ1 interaction site Y816, but not at Y515 (Fig. 1C,D) in fibroblasts. To investigate the effect of this mutation on TRKB dimerization, we used split luciferase protein complementation assay in neuroblastoma cells (Merezhko et al., 2020). We observed that although the basal TRKB dimerization was not affected, the Y433F mutation compromised BDNF-induced increase in dimerization of TRKB (Fig. S1G). Furthermore, translocation of TRKB.Y433F to lipid rafts was reduced when compared to the wild type TRKB (Fig. S3I). In agreement with the previous observation (Pereira and Chao, 2007), the BDNF-induced increase in the interaction of TRKB with raft-restricted FYN was compromised (Fig. 1E). Taken together, these data indicates that cholesterol interacts with a CARC domain within the TRKB TM region and promotes TRKB translocation to lipid raft-like regions on neuronal surface, thereby promoting BDNF signaling.

Modeling of cholesterol-TRKB interaction

We next used molecular dynamics simulations (MD) to investigate the atomistic-scale organization of TRKB TM domain dimers (Table S1). In low cholesterol concentrations, extensive docking calculations revealed five possible dimer structures. However, MD simulations showed that only one of the structures is stable in phosphatidylcholine bilayer with 20-40 mol% cholesterol. This structure matches a cross-like conformation, where the coupling between the two TM domains takes place at ^{439}AXXXG^{443} (Fig. 1F-H), which conforms to the known GXXXG-like dimerization motif (Li et al., 2012; Senes et al., 2004). This cross-like conformation is analogous to that proposed for the TM domains of EGF receptor dimer, where the distance between the C-termini of TM domains largely determines the orientation of the intracellular domains and EGF signaling (Arkhipov et al., 2013; Endres et al., 2013; Sinclair et al., 2018). In the absence of cholesterol, the average distance between the TRKB TM C-termini was 19.4Å on average (Fig. S2). However, when the TM dimer was simulated at a higher cholesterol concentrations, the dimer conformation switched from the stable cross-like structure seen at 20mol% (with the average C-terminal distance of 14.3Å) to a more parallel conformation at 40mol% (the average C-terminal distance decreased to 12.4Å). Extensive analysis and complementary simulations revealed that the main factor causing the change in the TM dimer structure in response to higher cholesterol concentration is the increase in membrane thickness (Fig. S2A) that enforces the TM domains to reduce their tilt to match the hydrophobic membrane thickness (Fig 1F-H).

The Y433F mutation on the TM dimers disrupted the tyrosine-tyrosine bond between monomers at Y433 (Fig. 1I) and forced a 40 degrees rotation relative to each other, compromising the contact at the dimerization motif GXXXA, and substantially reducing the C-terminal distance of the TM domains (Fig. S2A). Taken together, these findings are consistent with our experimental data showing that there is an optimal cholesterol concentration for TKRB function, with a compromised function at low cholesterol

concentrations where the structure of the TM domain is likely disrupted (Arkhipov et al., 2013) and at high concentrations where the cross-shaped TM structure is replaced with a presumably instable parallel TM orientation.

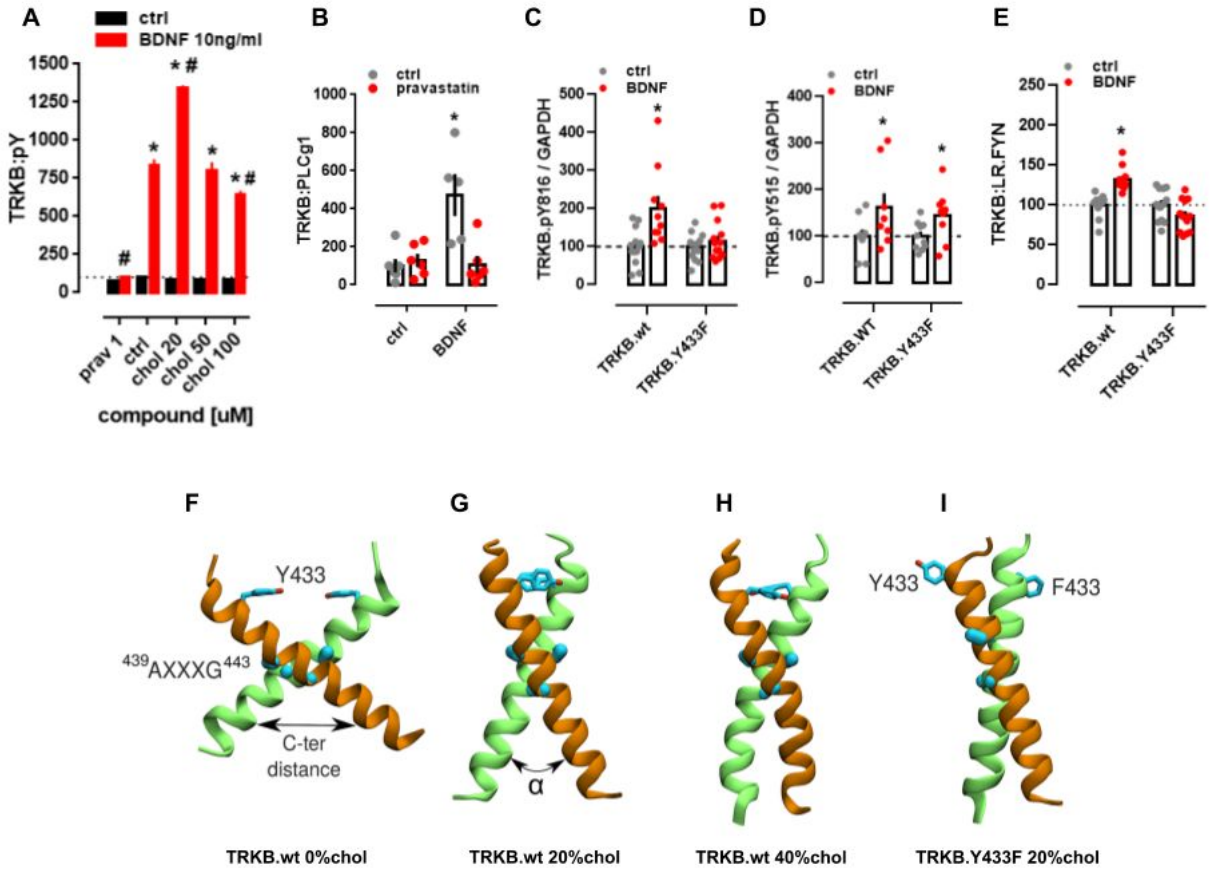

Figure 1. Identification of cholesterol-interacting motif (CARC) in TRKB. (A) Dual effect of cholesterol in BDNF-induced activation of TRKB [interaction: F(5,84)=5.654, p=0.0002; n=6/group]. (B) BDNF-induced increase in TRKB:PLC-γ1 is prevented by previous treatment with pravastatin [interaction: F(1,19)=11.23, p=0.003; n=5-6]. (C) BDNF-induced phosphorylation of TRKB at Y816 is prevented in the TRKB.Y433F mutant [interaction: F(1,47)=6.688, p=0.0129; n=10-14]. (D) The Y433F mutation does not affect BDNF-induced phosphorylation of TRKB at Y515 residues in MG87 cells [interaction: F(1,33)=0.1874, p=0.6679; n=9-10]. (E) The BDNF-induced increase in TRKB interaction with FYN fragment in lipid raft is compromised by the Y433F mutation [interaction: F(1,44)=20.96, p<0.000; n=12]. * p<0.05 from the ctrl/ctrl group, data expressed as Mean±SEM of percentage from control group. Structures for wild-type TRKB in the absence of cholesterol (F) and at cholesterol concentrations of (G) 20mol% and (H) 40mol%, and (I) for the TRKB.wt and TRKB.Y433F heterodimer at 20mol% (systems 1-4, Table S1, Fig. S2 for distance and α values between C-termini).

Antidepressants bind to TRKB CARC domain

We and others have previously shown that essentially all antidepressant drugs promote TRKB signaling in the rodent brain and that TRKB signaling is required for their behavioral effects of antidepressants in rodents (Castrén and Antila, 2017; Monteggia et al., 2004; Saarelainen et al., 2003). Many antidepressant drugs are cationic amphipathic molecules that share many features with cholesterol and they are known to interact with phospholipids and accumulate to lipid rafts (Chen et al., 2012; Erb et al., 2016;

Kornhuber et al., 1995; Wray et al., 2018). We therefore speculated whether antidepressants might also interact with the TRKB CARC domain. We found that several antidepressants mimicked the effects of cholesterol and enhanced the interaction of TRKB and the pTRKB.Y816 with PLC-γ1 in primary cortical neurons (Fig. S3A-H). This interaction was blocked by the cholesterol-sequestering agent β-cyclodextrin - βCDX (Fig. S3A-F), indicating that increased TRKB signaling induced by antidepressants is modulated by cholesterol. Furthermore, the SSRI fluoxetine increased the surface expression of TRKB in cortical neurons, and this effect was also prevented by βCDX (Fig. S3F). These data suggest that antidepressants interact with the TRKB cholesterol interaction motif.

We then assayed for the binding of antidepressants to TRKB. We first found that biotinylated fluoxetine binds to immunoprecipitated TRKB with a relatively low μM affinity (Kd=2.42μM; Fig. 2A). To verify the direct interaction between fluoxetine and TRKB, we used microscale thermophoresis assay - MST (Jerabek-Willemsen et al., 2014). This assay confirmed that N-terminally GFP-tagged TRKB derived from lysates of transfected HEK293T cells bound to unlabeled fluoxetine (Fig. S4D). We further found that tritiated imipramine binds to TRKB at micromolar affinity (Kd=1.43μM; Fig. 2B) similar to that seen with fluoxetine. Although the affinities of imipramine and fluoxetine to serotonin transporter (5HTT) are orders of magnitude higher than those observed for TRKB, micromolar affinity corresponds well to the concentrations of antidepressant reached in the human brain during chronic treatment (Bolo et al., 2000; Henry et al., 2000; Karson et al., 1993; Kornhuber et al., 1995). Binding of biotinylated fluoxetine (1μM) to TRKB was displaced by unlabeled fluoxetine (Ki=1.69μM, Fig 2D) but also by imipramine, ketamine, esketamine and R,R-HNK (Ki=1.03, 12.30, 2.86 and 2.23μM, respectively; Fig 2E-H). By contrast, control compounds isoproterenol, chlorpromazine, diphenhydramine and 2S,6S-HNK that are structurally and physico-chemically similar to antidepressants, produced weak, if any displacement of biotinylated fluoxetine (Fig. S4B,C). As expected, BDNF failed to displace fluoxetine from TRKB (Fig. S4A), consistent with different sites for TRKB interaction with antidepressants and BDNF.

The finding that ketamine and R,R-HNK compete with fluoxetine indicates that not only typical antidepressants, but also the novel rapid-acting antidepressants might bind to TRKB. Remarkably, R,R-HNK clearly bound to TRKB (Kd=1.82μM, Fig. 2C). Recent findings indicate that R,R-HNK produces antidepressant-like effects in rodents at concentrations that do not inhibit NMDA receptors, the proposed primary interaction site for rapid-acting antidepressants (Zanos et al., 2016, 2018). However, no alternative binding site for R,R-HNK that could explain its antidepressant-like effects was identified. Our current finding now suggests that TRKB might be the so far elusive direct target for R,R-HNK.

To investigate whether the TRKB CARC domain is involved in antidepressant binding, we assayed binding to the TRKB.Y433F mutated receptor. The affinity of fluoxetine, imipramine and R,R-HNK to TRKB.Y433F was much lower than to the wild-type TRKB (Fig. 2A-C), reinforcing that the binding may take place at the TRKB CARC site. Together, these results suggest that all of the investigated

antidepressants interact with the TRKB CARC motif at clinically meaningful concentrations (Bolo et al., 2000; Henry et al., 2000; Karson et al., 1993; Kornhuber et al., 1995).

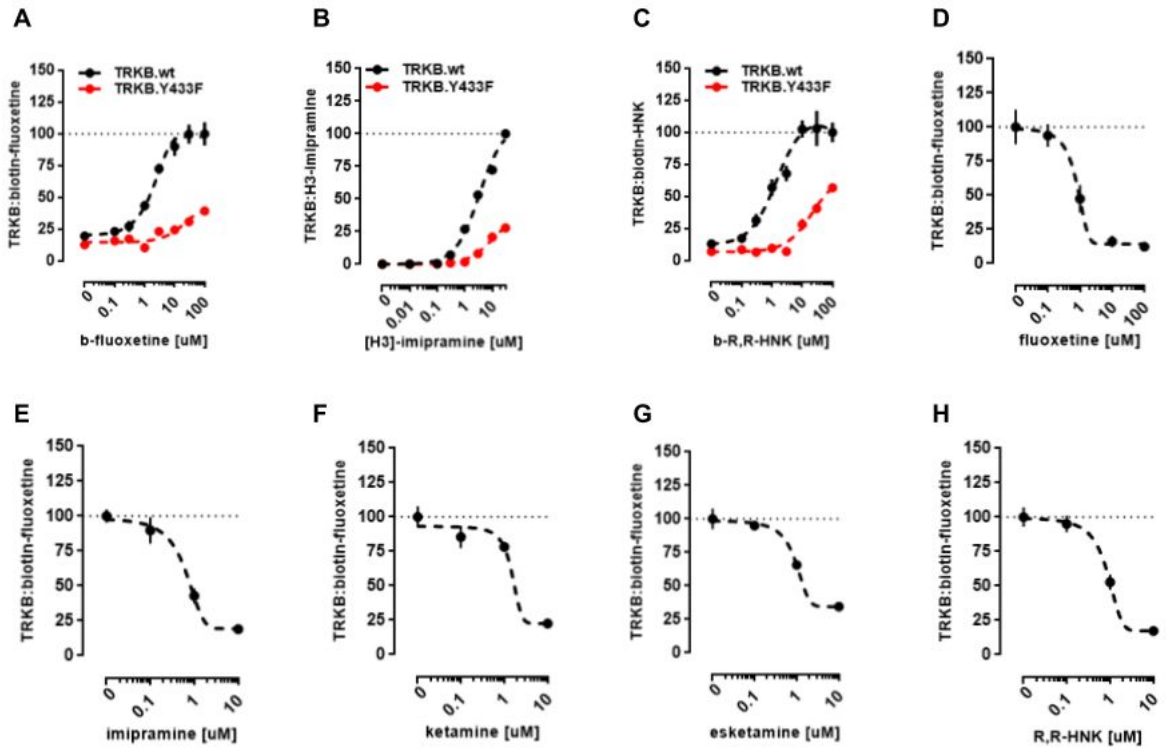

Figure 2. Binding of antidepressants to TRKB. Binding of (A) biotinylated fluoxetine [interaction: $F(7,153) = 16.18$, $p < 0.0001$; n=6-14], (B) tritiated imipramine [interaction: $F(7,16) = 106.1$, $p<0.0001$; n=2] and (C) biotinylated R,R-HNK [interaction: $F(7,160)=14.91$, $p<0.0001$; n=6-14] to precipitated TRKB.wt or TRKB.Y433F. Data expressed Mean±SEM of percentage of binding at 100µM for fluoxetine and R,R-HNK or at 30µM for imipramine. Biotinylated fluoxetine (1µM) interaction with TRKB is reduced by (D) fluoxetine, (E) imipramine, (F) ketamine, (G) esketamine and (H) R,R-HNK (n=8/group).

Modeling fluoxetine binding to TRKB

We next employed a combination of docking and molecular dynamics simulations to characterize the putative antidepressant binding site using fluoxetine as the model drug. The transmembrane helix dimer features four distinct v-shaped crevices around the central hinge region. We first docked fluoxetine separately to each of the four crevices using 30 different crisscrossed conformations of TRKB TM dimers, each separately obtained by independent 1 microsecond-long MD sampling in 20mol% cholesterol membrane. We then combined the decoys from all docking runs and evaluated them based on the interface score. The best scoring configurations consistently featured fluoxetine binding to the crevice facing the extracellular site in a common binding mode (Fig. 3A).

To further assess the binding mechanism of fluoxetine and verify the drug binding site in a more native-like environment, we performed 120 MD simulations each initiated from a different configuration obtained by repositioning the drug in the vicinity of the characterized binding pocket and randomizing its

orientation. While the drug could re-establish the characterized binding pose in some simulations for a brief time, only one out of 120 simulations resulted in long-lasting stable association with the protein. Inspection of the simulation trajectories revealed that the stable drug binding not only engages several protein residues (Fig. 3A,C,D) important for the dimerization and proper orientation of the helices, but also recruits phospholipids (Fig. 3B).

We next modeled the effects of cholesterol-regulated membrane thickness on fluoxetine binding to TRKB. As shown above, the configuration of TRKB TM dimers was stable at 20mol% of cholesterol, but the increased membrane thickness at 40mol% of cholesterol destabilized the structure (Fig. 1G,H). We found that even at 40mol% of cholesterol, fluoxetine promoted the retention of TRKB dimers in the active configuration, close to the one observed in 20mol%, thus maintaining the separation between the C-termini, which is consistent with our biochemical observations (Fig. 1A). Following drug expulsion, the simulations invariably transitioned to the more parallel conformation seen in Fig. 1H. These data suggest that fluoxetine binding to the dimeric TRKB interface acts as a wedge, stabilizing the cross-shaped active conformation at high cholesterol concentration typically present in synaptic membranes.

We also investigated the effect of the Y433F mutation on fluoxetine binding *in silico*. Starting with equilibrated stable protein-fluoxetine complex systems, we introduced the Y433F mutation in 20 independent simulations. The drug left the binding pocket in all simulations within a short time-frame. Indeed, the residence-time of the drug is decreased by at least 4 times upon the mutation (161ns) when compared to the wild-type protein (>696ns). These results indicate a strong destabilizing effect of the mutation on fluoxetine-TRKB interaction.

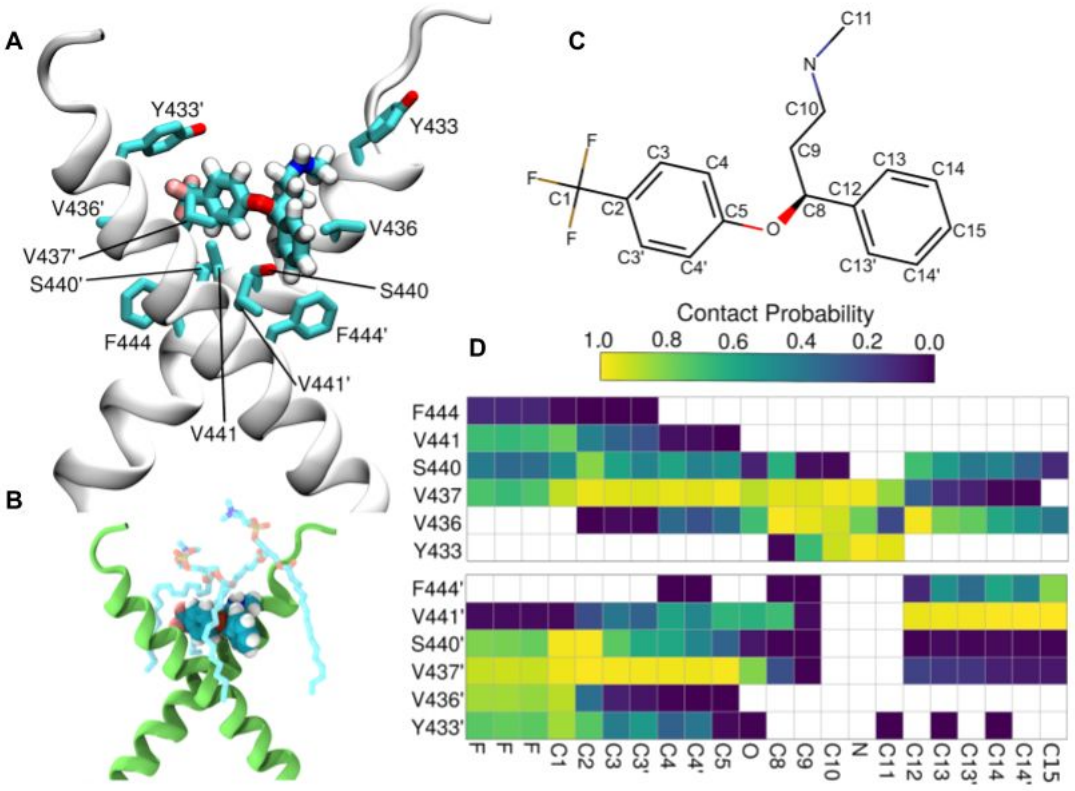

Figure 3. The fluoxetine binding pocket at the dimeric interface of the TRKB transmembrane helices. (A) A representative snapshot showing fluoxetine in the crevice between the TRKB monomers. Fluoxetine including its hydrogens is shown in licorice representation and the protein in cartoon representation. The side chains that interact with the drug are labeled and also shown in licorice. (B) Fluoxetine binding also involves lipid molecules, which provide a closed cavity for the drug. The protein is shown in green cartoon representation, the drug in van der Waals representation, and the lipids in licorice representation. (C) The chemical structure of fluoxetine. The atom names are labeled and the chemically equivalent atoms are indicated with an apostrophe. (D) The contact probability between drug heavy atoms and the interacting protein residues are shown. The upper and lower panels correspond to the two different transmembrane helices (residues of the second helix are tagged with an apostrophe). Contact probabilities are calculated using a minimum distance cutoff of 5Å (System 9, Table S1).

TRKB CARC motif modulates TRKB trafficking

TRKB receptors are predominantly localized intracellularly in vesicles that are translocated to cell surface upon neuronal activation or BDNF exposure (Du et al., 2000; Haapasalo et al., 2002; Meyer-Franke et al., 1998). To investigate the effects of antidepressants on TRKB trafficking and surface expression, we first evaluated the mobility of TRKB in neuronal spines using fluorescence recovery after photobleaching (FRAP) assay. In hippocampal primary cultures (DIV14) transfected to express GFP-tagged TRKB, the fluorescence is rapidly recovered in neurite shafts after bleaching (Fig. S5A), however, very little recovery was seen in dendritic spines within the time frame of two minutes (Fig. 4A). When neurons were pretreated with BDNF (10ng/ml/15min) before bleaching, there was a rapid recovery of GFP-TRKB fluorescence, which indicates TRKB trafficking to dendritic spines (Fig. 4B,E). We then pretreated the cells with fluoxetine (1μM) to investigate whether antidepressants mimic the effects of BDNF on TRKB trafficking.

Indeed, fluoxetine, like BDNF, induced a rapid increase in the recovery of GFP-TRKB fluorescence in dendritic spines without any effect on dendritic shafts (Fig. 4C,F). Similarly, pretreatment with ketamine (10μM) also promoted recovery of GFP-TRKB fluorescence in dendritic spines (Fig. 4D,G). We then transfected cultured hippocampal neurons with GFP-tagged TRKB.Y433F (Fig. 4H-J). There was no difference in GFP-TRKB.Y433F expression in neurons before bleaching, indicating that TRKB.Y433F is expressed in neurons to the same extent as the wild-type TRKB. However, after photobleaching, neither BDNF, fluoxetine nor ketamine produced any increase in GFP-TRKB fluorescence in dendritic spines when compared to vehicle-treated cells (Fig. 4H-J). These data demonstrate that BDNF, fluoxetine and ketamine promote TRKB trafficking in dendritic spines and that this effect is dependent on the TRKB CARC domain.

We next investigated clustering of TRKB on plasma membrane using dSTORM/TIRF superresolution microscopy in fibroblast cell line transfected with either wild-type TRKB or the TRKB.Y433F mutant receptors, both tagged with GFP. We observed that both BDNF and fluoxetine increased the size of clusters of wild-type TRKB at the plasma membrane, indicating that the increased trafficking leads to increased cell surface expression of TRKB (Fig 4K,L). However, although the basal expression of GFP-TRKB.Y433F at cell surface was similar to that of the wild-type TRKB (Fig. 4M,N), BDNF and fluoxetine failed to promote clustering of GFP-TRKB.Y433F at the cell surface (Fig. 4O). Thus, TRKB translocation to and clustering at the plasma membrane promoted by BDNF (Haapasalo et al., 2002; Suzuki et al., 2004) or antidepressants (Fred et al., 2019) are dependent on the TRKB CARC domain.

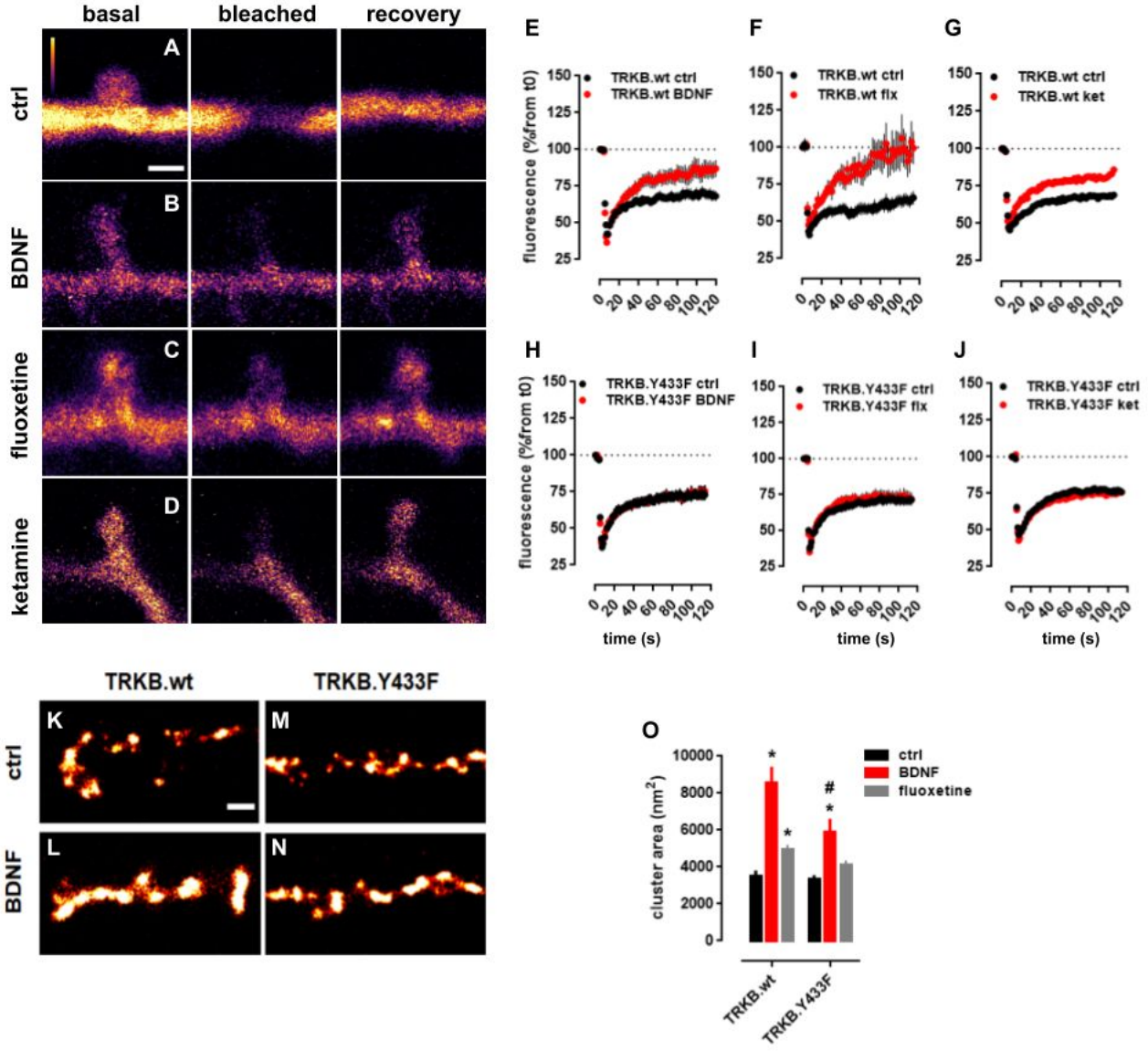

Figure 4. Effects of BDNF and antidepressants on TRKB trafficking. Representative images of the spine and shaft fluorescence in (A) control, (B) BDNF, (C) fluoxetine or (D) ketamine treated rat hippocampal neurons (E18; DIV14) transfected with GFP-TRKB before (basal), immediately (bleached) and 2 min (recovery) after photobleaching (for analysis of neurite shaft recovery see Fig. S5A). Scale bar: 1000nm. (E,H): BDNF [10ng/ml/15min, TRKB.wt n=17-27; interaction: $F(62,2604)=5.435$, $p=0.0001$; TRKB.Y433F n=27-39; interaction: $F(52,3328)=0.4595$, $p=0.99$], (F,I) Fluoxetine [10µM/15min, TRKB.wt n=9-22; interaction: $F(177,3068)=2.220$, $p=0.0001$; TRKB.Y433F n=28-42; interaction: $F(59,4012)=0.5555$, $p=0.99$] and (G,J) ketamine [10 µM/15min,TRKB.wt n=15-18; interaction: $F(59,1829)=3.361$, $p<0.0001$; TRKB.Y433F n=20-22; interaction: $F(59,2360)=0.3995$, $p>0.9999$] trigger the recovery of GFP-TRKB in dendritic spines but this is prevented in GFP-TRKB.Y433F expressing neurons; data expressed as mean±SEM of percentage from t=0. (K-N) Representative images of the BDNF-induced clusters of GFP-TRKB in the surface of MG87.TRKB cells. Scale bar: 250nm. (O) BDNF (10 ng/ml/15 min) and fluoxetine [10 µM/15min, TRKB.wt n=365-593; TRKB.Y433F n=232-547; interaction: $F(2,2717)=4.305$, $p=0.0136$] enhance the formation of clusters of GFP-TRKB on the surface of MG87.TRKB cells but not in the GFP-TRKB.Y433F expressing cells. *$p<0.05$ from respective control (vehicle-treated) groups; #$p<0.05$ from BDNF- or fluoxetine-treated wt group (Fisher's LSD), clusters from 10 cells/group, and 10 regions of interest (ROI) per image, mean±SEM of cluster area (nm^2).

TRKB CARC motif modulates synaptic plasticity

BDNF is known to be a critical mediator of synaptic plasticity and is required for long-term potentiation (LTP) in slices as well as *in vivo*, and these effects are mediated by TRKB (Ernfors and Bramham, 2003; Minichiello, 2009; Panja and Bramham, 2014). We therefore investigated whether interaction of cholesterol with TRKB is involved in BDNF-induced LTP. Infusion of BDNF into the dentate gyrus of anesthetized rats significantly increased synaptic strength, as previously reported (Messaoudi et al., 2002; Panja and Bramham, 2014) (Fig. 5A). However, this effect of BDNF was partially prevented when rats were co-treated with pravastatin (10mg/kg/day/14days; Fig. 5A), suggesting that neuronal cholesterol is required for the effects of BDNF on LTP.

To investigate whether this effect of BDNF on LTP involves the TRKB CARC motif, we generated a mouse carrying the TRKB.Y433F mutation. We first investigated the LTP in the CA3-CA1 synapse induced by theta-burst stimulation, which is known to be more dependent on BDNF than the stronger tetanic stimulation (Kang et al., 1997; Patterson et al., 2001). Theta-burst stimulation reliably induced an LTP in the CA3-CA1 synapse in slices derived from wild-type mice. Remarkably, similar stimulation of slices derived from heterozygous TRKB.Y433F mice failed to induce any potentiation (Fig. 5B), suggesting that TRKB CARC motif is critical for LTP. However, tetanic stimulation induced LTP in both wild-type and TRKB.Y433F slices (Fig. S5B), consistent with the central role of BDNF in theta-burst mediated LTP (Kang et al., 1997; Minichiello et al., 2002; Patterson et al., 2001). Taken together, these data indicate that interaction of cholesterol with the TRKB CARC domain is critical for synaptic plasticity induced by BDNF.

TRKB CARC motif mediates the behavioral effects of antidepressants

We next investigated whether TRKB-cholesterol interaction and antidepressant binding to TRKB influence neuronal plasticity-dependent learning and behavior. We first tested the effects of antidepressants on long-term memory using object location memory (OLM) test. Mice were allowed to explore two identical objects placed in different corners of the cage for 15min. After 7 days exposure to fluoxetine (15mg/kg/7days - 0.10mg/l - in the drinking water), mice were placed in a cage where one of the objects was placed to a different corner and exploration of that object relative to the stationary object was recorded. We observed that fluoxetine treatment improved the performance of wild-type mice in the OLM test (Fig. 5C). The behavior of vehicle-treated heterozygous TRKB.Y433F mice was similar to their vehicle-treated wild-type littermates, however, fluoxetine treatment failed to improve the behavior of mutant mice (Fig. 5C). A similar lack of response to fluoxetine was observed in BDNF haploinsufficient mice (Fig. S5E). We also tested the effect of fluoxetine in the OLM test in serotonin transporter knockout (5HTT.ko) mice lacking the primary site of action of SSRIs. Remarkably, these mice respond to fluoxetine treatment normally in the OLM test (Fig. S5F), indicating that the effects of fluoxetine in this test are not mediated by inhibition of serotonin transport. This is consistent with the recent finding that the behavioral and electrophysiological

effects of SSRIs are preserved in 5HTT.ko mice (Normann et al., 2018). However, a recent study found that behavioral effects of fluoxetine are lost in mice with a point mutation in 5HTT that impairs the response to antidepressant drugs (Nackenoff et al., 2016).

Forced swim test (FST) is the classical behavioral test used for evaluating antidepressant potential. Previous studies have shown that BDNF-TRKB signaling is sufficient and necessary for the effects of antidepressants in this test (Koponen et al., 2005; Lindholm and Castrén, 2014; Monteggia et al., 2004; Saarelainen et al., 2003). As expected, we found that chronic treatment of wild-type mice with fluoxetine (15mg/kg/21days in the drinking water) significantly reduced immobility in the FST (Fig. 5E). Similarly, a single injection of the fast-acting antidepressant ketamine (10mg/kg i.p., 2h before test) significantly reduced immobility (Fig. 5F). In contrast, both fluoxetine and ketamine were ineffective in TRKB.Y433F mice (Fig. 5E,F).

We further investigated the effects of fluoxetine on fear extinction in wild-type and TRKB.Y433F mutant mice, as fluoxetine is known to promote extinction of conditioned fear BDNF-dependently (Andero and Ressler, 2012; Deschaux et al., 2011; Karpova et al., 2011). The freezing response was indistinguishable between the genotypes after conditioning (Fig. 5D). As previously observed (Karpova et al., 2011), fluoxetine (in the drinking water for 2 weeks) promoted extinction of conditioned fear in wild-type mice (Fig. 5D). There was an unexpected increase in the freezing response in TRKB.Y433F mice after the first extinction session before a partial extinction seen after the second session. However, fluoxetine did not have any effect on freezing in TRKB.Y433F mice at any time point (Fig. 5D).

Finally, we investigated the interaction between TRKB and antidepressant on ocular dominance (OD) plasticity in the visual cortex, a standard method of cortical plasticity (Wiesel, 1982). Monocular deprivation for a week induces a shift in OD during a critical period, but not in adults (Wiesel, 1982). It has been reported, however, that chronic fluoxetine treatment reactivates a critical period-like plasticity in the visual cortex of adult mice, allowing an OD shift in response to deprivation to develop (Maya Vetencourt et al., 2008; Steinzeig et al., 2017). We assessed ocular dominance using optical imaging of intrinsic signal (Cang et al., 2005; Greifzu et al., 2011; Steinzeig et al., 2017). As reported before, when mice were treated with fluoxetine for 4 weeks (in drinking water), a 7-day monocular deprivation during the last treatment week induced a dramatic shift in OD in favor of the open eye (Fig. 5G). We now observed that a significant shift in OD comparable to that produced by fluoxetine was observed when mice were treated with R,R-HNK, but a much shorter treatment was needed for R,R-HNK (10mg/kg, ip, three injections in alternate days right before and during the 7-day deprivation) than for fluoxetine (Fig. 5G), consistent with the fast action of R,R-HNK. Ketamine (10mg/kg, ip, three injections in alternate days right before and during the 7 d deprivation), also permitted a significant OD shift, however, the magnitude of this shift was lower than that produced by fluoxetine and R,R-HNK. Remarkably, the effect of fluoxetine on the shift in ocular dominance

was lost in TRKB.Y433F heterozygous mice (Fig. 5H), indicating that the plasticity-inducing effects of antidepressants may be mediated by their direct binding to TRKB.

Taken together, these data demonstrate that the behavioral effects produced by different antidepressants were lost in TRKB.Y433F mutant mice. Moreover, we also observed that the behavioral effects were lost when antidepressants were co-administered with pravastatin (Fig. S6), demonstrating that TRKB interaction is cholesterol-dependent and not produced by any non-specific effects of the TRKB.Y433F mutation.

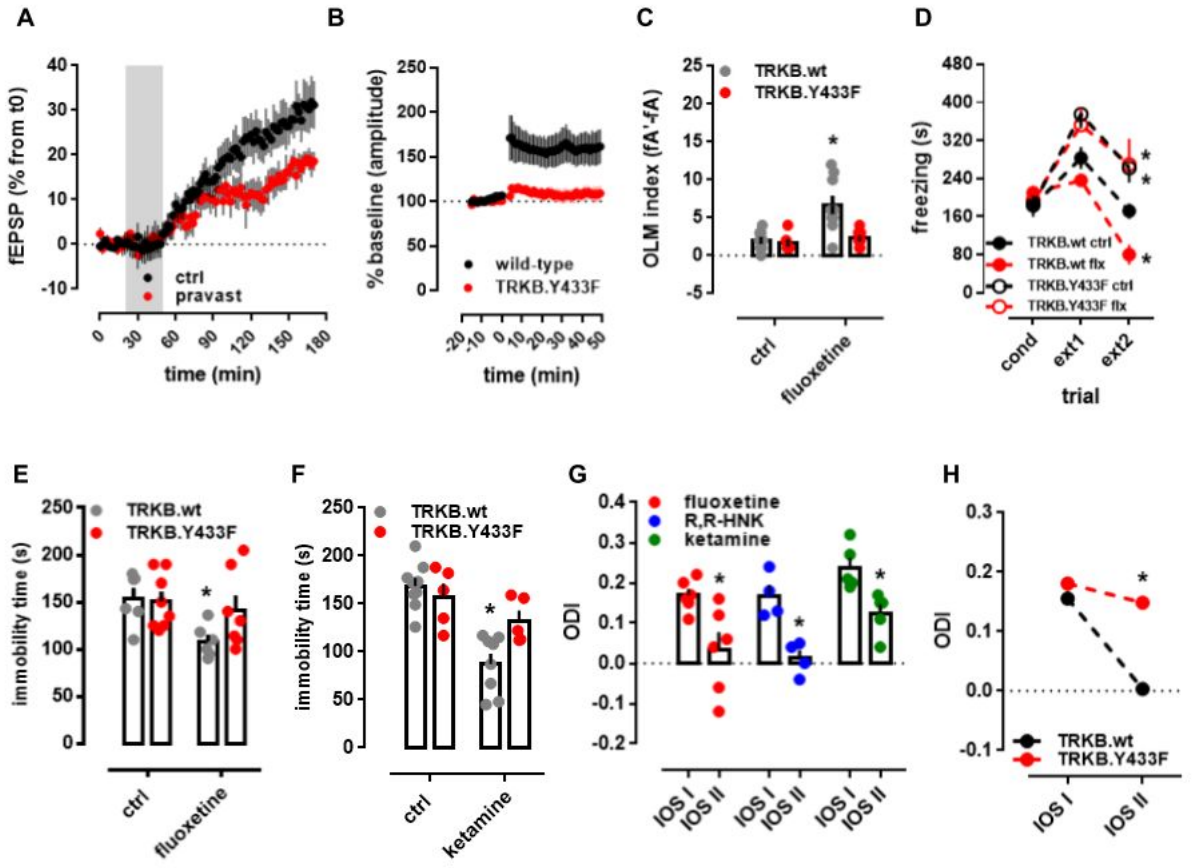

Figure 5. Role of TRKB CARC in drug induced plasticity. (A) BDNF-induced LTP in rat dentate gyrus is attenuated by pravastatin administration [n=8-9; interaction: F(85,1290)=1.484, p=0.0036]. (B) Theta-burst induced LTP in the CA3-CA1 synapses of hippocampal slices from wild-type mice, but not in slices from Y433F mutant mice [interaction: F(61,610)=5.466, p<0.0001] from baseline [in A t=0; in B t=-20min]. (C) Fluoxetine improved object location memory (OLM) in wild-type mice, but this effect was absent in the TRKB.Y433F mice [interaction: F(1,18)=6.878, p=0.017; n=8-9]. (D) Fluoxetine facilitated the extinction of contextual conditioned fear in the 8 min session, and this response is blocked in mice carrying the TRKB.Y433F mutation [interaction: F(6,34)= 3.241, p= 0.0126; n=5-6] . (E) fluoxetine [treatment: F(1,23)=5.433, p=0.0289; n=6-8] and (F) ketamine [treatment: F(1,23)=24.26, p<0.0001; n=5-9] reduce immobility in the forced swim test in TRKB.wt mice, but are ineffective in TRKB.Y433F mutants. (G) Fluoxetine (10mg/kg/day/28days - 0.08mg/l; po; n=6), R,R-HNK (10mg/kg ip injection every second day for 6 days, n=4) and ketamine (10mg/kg ip injection every second day for 6 days, n=5) permitted a shift in ocular dominance in adult mice during 7 days of monocular deprivation [paired t test: flx: t(5)=2.985, p=0.0306; R,R-HNK t(3)=6.875, p=0.0063; ket: t(4)=6.517, p=0.0029]. *p<0.05 between intrinsic signal imaging (IOS) sessions before and after monocular deprivation (Fisher's LSD), mean±SEM of ocular dominance index (ODI). (H) Fluoxetine fails to permit a shift in ocular dominance in TRKB.Y433F mice [n=6-7; interaction: F(1,19)=107.9, p<0.0001]. *p<0.05 from the control group in the same session, Fisher's LSD. Data expressed as Mean±SEM.

Discussion

In this study, we have identified a novel cholesterol-interaction motif in the BDNF receptor TRKB and shown that cholesterol promotes and is needed for TRKB signaling. Molecular modeling and simulations proposed a novel model for the configuration of TRKB TM domains and revealed how cholesterol regulates this configuration through membrane thickness. Given the major role of BDNF-TRKB signaling in synaptic stabilization and plasticity (Park and Poo, 2013), these data suggest that interaction with TRKB may mediate at least a part of the well-known plasticity-enhancing effects of cholesterol (Martin et al., 2014; Mauch et al., 2001; Pfrieger and Ungerer, 2011).

We have then shown that several different antidepressants, including an SSRI fluoxetine, tricyclic imipramine, rapid-acting ketamine and its metabolite R,R-HNK bind to TRKB transmembrane helices with a therapeutically relevant affinity. Molecular simulations revealed a binding pocket for fluoxetine formed by the dimerization of TRKB transmembrane helices. Antidepressant binding stabilizes the TRKB transmembrane domain structure in high cholesterol-containing membranes, such as synaptic membranes, and thereby allosterically promotes TRKB membrane localization and BDNF signaling. A mutation in the TRKB cholesterol-interaction motif reduces antidepressant binding and compromises the plasticity-promoting effects of BDNF and antidepressants *in vitro* and *in vivo*. Taken together, our study represents a substantial step forward in understanding the molecular mechanisms of how cholesterol and antidepressant drugs regulate neuronal plasticity.

TRKB-cholesterol interaction

Astrocyte-derived cholesterol has been recognized as an important regulator of neuronal maturation and plasticity (Martin et al., 2014; Mauch et al., 2001; Pfrieger and Ungerer, 2011), but the mechanisms through which cholesterol acts to produce these effects have remained unclear. The recent recognition of the CRAC/CARC sequences in several proteins interacting with cholesterol (Fantini and Barrantes, 2013) has facilitated the identification of proteins that potentially mediate the effects of cholesterol in cells. We have here demonstrated that TRKB possesses a CARC domain and that cholesterol potentiates the effects of BDNF on TRKB signaling.

Cholesterol is known to regulate BDNF signaling (Pereira and Chao, 2007; Suzuki et al., 2004; Zonta and Minichiello, 2013), and BDNF, in turn, promotes neuronal cholesterol synthesis (Suzuki et al., 2007). Synaptic membranes are enriched in cholesterol and resemble cholesterol-rich lipid rafts (Ikonen, 2008). TRKB normally resides outside rafts, but it can transiently translocate to rafts upon BDNF stimulation (Pereira and Chao, 2007; Suzuki et al., 2004), as also observed here. This translocation takes place rapidly and may be related to our observation of TKRB trafficking to dendritic spines and clustering on plasma membrane, both of which were stimulated by BDNF and antidepressants. Translocation of TRKB to rafts is dependent on Fyn kinase (Pereira and Chao, 2007; Suzuki et al., 2004) and we observed that

BDNF increases interaction of Fyn with wildtype TRKB, but not with the TRKB.Y433F mutant. These data suggest a scenario where activation of TRKB with BDNF or antidepressants promotes its translocation to cholesterol-rich synaptic membranes.

TRKB appears to be the only member of the TRK family of neurotrophin receptors that contains a CARC motif in the TM domain. Although TRK family members show high homology, the TM domain of TRKB differs from that of TRKA and TRKC. TRKA and TRKC act as dependence receptors inducing cell death in the absence of a ligand, but TRKB does not have this property (Nikoletopoulou et al., 2010). There is data to suggest that this property is dependent on the transmembrane domain, and a chimeric TRKB with the TM domain of TRKA resides in rafts and mediates death in the absence of BDNF (Dekkers et al., 2013). Our data suggest that the evolution of TRKB to include a CARC motif as a cholesterol sensor may be important for its function as mediator of activity-dependent plasticity.

Our modeling data implicates that the major effect of cholesterol on TRKB function is mediated by cholesterol-induced changes in the membrane thickness, which alters the relative orientation of TRKB dimers. This is consistent with our observation that cholesterol plays a permissive role in BDNF-induced TRKB activation, but high cholesterol concentrations limit BDNF signaling. Little is known about the structure of TRKB dimers in biological membranes. Our simulation data now suggest that TM domains of TRKB cross each other at ^{439}AXXXG^{443} dimerization motif and that membrane thickness critically regulates the structure and function of dimerized TRKB. Previous studies have recognized a similar kind of crossed structure for epidermal growth factor (EGF) receptor TM dimers and shown that the distance of the C-terminal ends of TM domains crucially determines the signaling capacity of the EGF receptor (Arkhipov et al., 2013; Endres et al., 2013; Sinclair et al., 2018). Although the exact structure of TRKB, encompassing the extracellular, TM and intracellular domains, remain to be determined, our data suggest that, analogous to the EGF receptor, the angle between the dimerized and criss-crossed TRKB TM domains, regulated by the membrane thickness, plays an important role in TRKB signaling. Specifically, our data suggest that in thick, cholesterol-rich membranes that are typically found in synapses and lipid rafts, TRKB TM domains assume a near-parallel position that presumably is not stable. This leads to the exclusion of TRKB from synaptic membranes and limits synaptic TRKB signaling. Furthermore, our modeling and simulation data suggest that binding of fluoxetine to a site formed by the crossed TM domains act as a wedge, maintaining a more stable structure in synaptic membranes, thereby allosterically facilitating BDNF signaling. Obviously, the configuration of the TM domain is not the only determinant of TRKB signaling capacity, nevertheless, we consider that our findings are a major step forward in understanding the interaction of TRKB with cellular membranes.

Antidepressant binding to TRKB

BDNF signaling is known to be crucial to the action of essentially all antidepressant drugs (Autry and Monteggia, 2012; Castrén and Antila, 2017; Duman and Monteggia, 2006), but this effect has been

assumed to be indirectly mediated by other proteins such as 5HTT or NMDA receptors. We now show that antidepressants bind to the transmembrane region of TRKB dimers with a therapeutically relevant affinity (Bolo et al., 2000; Karson et al., 1993), stabilizing a conformation of the TRKB TM dimers favorable for signaling, thereby promoting TRKB translocation to and retention at the plasma membrane, where it is accessible to BDNF. Specific binding was observed not only by fluoxetine and imipramine, representing typical SSRI and tricyclic antidepressants, respectively, but also by the rapid-acting ketamine metabolite RR-HNK. Binding of labeled fluoxetine was displaced by fluoxetine itself and by imipramine, RR-HNK and also by ketamine, which suggests that these drugs bind to at least partially overlapping binding sites. However, several structurally similar molecules showed little if any capacity to displace fluoxetine binding, suggesting specificity for this binding site.

Atomistic simulations identified a candidate binding site for fluoxetine at the outer opening of the crossed dimer of TRKB TM domains, and suggested a plausible mechanisms for how this binding may stabilize TRKB dimers in a favorable conformation and thereby promote the localization of TRKB at synaptic membranes and allosterically enhance BDNF effects. Simulations predict and mutagenesis demonstrates that the CARC motif plays a critical role in the binding of antidepressants to TRKB. Taken together, these data suggest that direct binding to the dimer of TRKB TM domains may function as a novel binding site for several different antidepressants. Simulations also predict that membrane lipids participate in fluoxetine binding to TRKB. Furthermore, our recent findings indicate that TRKB exists as a multi-protein complex that also includes transmembrane proteins (Fred et al., 2019). It is therefore possible that other proteins and lipids participate in antidepressant binding to TRKB in cell-type and subcellular compartment dependent manner. Nevertheless, further characterization of this binding site may yield important information for discovery of new antidepressants with increased potency for plasticity-related behavioral effects.

The affinity of ketamine to TRKB is comparable to its affinity to NMDA receptors, but fluoxetine and imipramine bind to 5HTT with a much higher affinity than to TRKB. Remarkably, however, micromolar concentrations of SSRIs are reached and apparently required in the brain during chronic treatment (Bolo et al., 2000; Henry et al., 2000; Karson et al., 1993; Kornhuber et al., 1995). The fact that concentrations (orders of magnitude higher than those required for binding to monoamine transporters) are achieved in the human brain has received surprisingly little attention.

It has been known for decades that the clinical antidepressant response to SSRIs and tricyclic antidepressants is only reached after several weeks of treatment, but the underlying reason for this delay has remained a mystery. One explanation has been that the process of neuronal plasticity induced by antidepressants may take time to develop. However, the discovery of the rapid action of ketamine, which is also dependent on plasticity, has undermined this explanation. Interestingly, micromolar brain concentrations of typical antidepressants are not achieved immediately upon administration, but the drugs

gradually accumulate in the brain during chronic treatment, reaching a plateau after several weeks of continuous treatment (Bolo et al., 2000; Henry et al., 2000; Karson et al., 1993; Kornhuber et al., 1995). These data suggest that the clinical response to antidepressants is only achieved after a brain concentration of a drug reaches the level to fill a low-affinity binding site, such as that of TRKB. Ketamine, on the other hand, being an anesthetic, may readily penetrate the brain and achieve a sufficient synaptic concentration quickly. Therefore, the gradual increase in brain concentration to a level needed for TRKB binding might be at least one explanation for why typical antidepressants take so long to act, while the rapid brain penetration of ketamine and RR-HNK enables fast action.

The present findings demonstrate that antidepressants bind to TRKB and thereby allosterically increase BDNF signaling. These findings directly link the effects of antidepressants to neuronal plasticity (Castrén and Antila, 2017). Juvenile-like plasticity induced by these drugs in the adult brain facilitates beneficial re-adaptation of neuronal networks that have been abnormally wired during development or by stress, which may explain the superiority of the combination of antidepressant treatment with psychotherapy (Pampallona et al., 2004). Our data suggests a new framework for antidepressant action where the drugs bind to the cholesterol-interaction site of TRKB, thereby allosterically promoting BDNF-induced plasticity, which is permissive for the activity-dependent network rewiring that underlies the clinical antidepressant response.

Acknowledgements: The authors would like to thank Sulo Kolehmainen and Seija Lågas (Neuroscience Center - UH), Marc Baumann and Rabah Soliymani (Department of Biochemistry and Developmental Biology - UH); and the Biomedicum Imaging Unit (BIU) at the University of Helsinki for technical help and Katja Kaurinkoski for language revision. We also thank Drs. Todd Gould (U. of Maryland) and Craig Thomas (NIH) for kindly supplying the R,R-HNK used in this study, Henri Huttunen (UH) for supplying GLuc-coupled raft-restricted FYN construct; and Yves-Alain Barde, Maija Castrén, Heikki Ruskoaho for their insightful comments to the present manuscript.

Funding: Castrén lab was supported by the ERC grant #322742 - iPLASTICITY; EU Joint Programme - Neurodegenerative Disease Research (JPND) CircProt project #301225 and #643417, Sigrid Jusélius Foundation, Jane and Aatos Erkko Foundation, and the Academy of Finland grants #294710 and #307416. Bramham lab was supported by the EU Joint Programme - Neurodegenerative Disease Research (JPND) CircProt project #30122. Lauri lab was funded by the Academy of Finland grant #297211. Vattulainen group was supported by the Academy of Finland (Center of Excellence) #307415, Sigrid Juselius Foundation, Helsinki Institute of Life Science, and CSC - IT Center for Science (computing resources). Normann and Serchov lab was funded by the German Research Council (#SE 2666/2-1) and the Forschungskommission of the Medical Faculty of the University of Freiburg (#SER1149/17). Saarma lab was funded by Jane and Aatos

Erkko Foundation. None of the funders had a role in the data acquisition and analysis, or manuscript preparation.

Authors contributions: PCC, CB, IV and EC designed the experiments; PCC, SMF, CAB, VK and CB performed the biochemical experiments with the assistance of LL and IC. MG, GE, TR and IV performed the molecular modeling and simulation experiments. RM and CAB performed the imaging experiments; CC, HA and AS performed intrinsic optical imaging experiments; FW, SP, and SL performed the electrophysiology experiments. PCC, CRAFD, CC, SV, and TS performed the behavioral studies; PCC and EC wrote the manuscript, with the help of MG, TR, CRB, CN, MS and IV.

Competing interests: EC received lecture fees from Janssen-Cilag. All other authors declare no conflict of interest.

Methods

Protein-protein and ligand docking: For simulations, the secondary structure prediction and modeling of the transmembrane domain of TRKB (residues 427-459) were performed using the FMAP (Folding of Membrane-Associated Peptides) server (Lomize et al., 2018). The initial models of the TRKB transmembrane (TM) (amino acids 427-459) dimers for atomistic MD simulations were generated using the MPDock application of the Rosetta software suite (Alford et al., 2015). The drug-binding pocket was characterized by local docking of the drugs to the TRKB TM dimers using the RosettaScripts interface (Fleishman et al., 2011).

Molecular Dynamics simulations. All atomistic simulations were performed using Gromacs 2018 (Abraham et al., 2015) employing the Charmm36(m) force field for the protein (Huang et al., 2017) and lipids (Klauda et al., 2010), the TIP3P water model (Jorgensen et al., 1983), and a compatible ion parameter set (Beglov and Roux, 1994). Drug parameters were generated using the CHARMM General Force Field (CGenFF) program (Vanommeslaeghe et al., 2009). Lipid membranes were comprised of POPC with a varying concentration of cholesterol (0, 20, 40 mol%). All production simulations (Table S1) were performed at two different temperatures (310 K, 363 K) in the NpT ensemble at a pressure of 1 atm, complemented by NVT simulations; key data and conclusions are based on simulations done at 310 K. All protein-membrane systems were constructed using CHARMM-GUI (Jo et al., 2008), and all simulation parameters were chosen as suggested.

Free energy calculations. All free energy calculations were performed using the free energy perturbation (FEP) method with Hamiltonian replica exchange. The free energies and their statistical errors were estimated with the Multistate Bennett Acceptance Ratio (MBAR) method using the Alchemical Analysis and the pymbar software (Klimovich et al., 2015). The necessary corrections arising due to the added restraints and the decoupled intra-molecular interactions were applied to obtain the final free energy values.

Analysis. All simulations were repeated through several replicas and the total simulation time covering all simulations was >500 microseconds. All analyses of this data were performed using the tools available in Gromacs 2018 and VMD (Humphrey et al., 1996), together with in-house scripts and software. A detailed description of simulation systems and parameters is given in the supplement file.

Animals: adult male rats were used for *in vivo* BDNF-induced LTP. Adult male and female mice (12-20 weeks): BDNF haploinsufficient, SERT.ko, TRKB.Y433F.het (detailed description in supplement), with respective wild-type littermates, were used in object-location memory, contextual fear conditioning or ocular

dominance plasticity. All animals were kept group housed with free access to food and water, except during the experimental sessions. All protocols were approved by local ethical committees (Finland: ESAVI/10300/04.10.07/2016; Norway: 6159; Germany: G-18-88).

Drugs and reagents: cholesterol, beta-cyclodextrin, pravastatin, fluoxetine, imipramine, ketamine, 2R,6R-HNK (R,R-HNK), 2S,6S-HNK, chlorpromazine, isoproterenol, diphenhydramine, BDNF, and NGF. The amino-biotinylation of fluoxetine, R,R-HNK and imipramine was performed using a commercial kit (EZ-Link NHS-PEG4 Biotinylation Kit, #21455, Thermo Scientific) and the reaction efficiency was evaluated by mass spectrometry. Antibodies: TRKB (R&D, #AF1494); PLC-γ1 (CST, #5690); pTRKB.Y515 (CST, #4619); pTRKB.Y816 (CST, #4168); pY (AbD Serotec, #MCA2472B); actin (Santa Cruz, #sc1615); GFP (Abcam, #ab290, #13970); flotillin-2 (CST, #3436); HRP-conjugated anti-Gt IgG (Invitrogen, #61-1620), anti-Rb IgG (BioRad, #170-5046); HRP-conj streptavidin (Thermo Fisher, #21126).

Cell culture and transfections: HEK293T (used for production of GFP-tagged TRKB), MG87.TRKB cells, Neuroblastoma-2A (N2A), and primary cultures of E18 rat embryos (DIV8 for biochemical analysis and DIV14 for FRAP) were cultivated according to previously described protocols (Antila et al., 2014; Fred et al., 2019; Sahu et al., 2019). The cells were transfected (DIV13 for hippocampal neurons) to express GFP- or Luciferase-tagged TRKB (wt or Y433F) or Luciferase-tagged FYN fragment, using lipofectamine 2000 according to manufacturer's instructions (#11668019, Thermo Fisher), or calcium phosphate co-precipitation (Xia et al., 1996), 24-48h prior to the experimental sessions or sample collection.

Determination of TRKB activation and coupling: the TRKB:pY (pTRKB), TRKB:pTRKB.Y816, TRKB:PLC-γ1 and PLC-γ1:pTRKB.Y816 interactions, and surface TRKB were determined by ELISA (Fred et al., 2019). Briefly, white 96-well plates (OptiPlate 96F-HB, Perkin Elmer) were coated with capturing anti-TRKB or anti-PLC-γ1 antibody (1:1000) in carbonate buffer (pH= 9.8) overnight (ON) at 4ºC. Following a blocking step with 2%BSA in TBS-T (2 h, RT), samples were incubated ON at 4ºC. The incubation with antibody against PLC-γ1, pTRKB.Y816 or pY (1:2000, ON, 4ºC) was followed by HRP-conjugated anti-Rb IgG (1:5000, 2h, RT) or HRP-conjugated streptavidin (1:10000, 2h, RT). For surface TRKB assay, the MG87.TRKB cells, cultivated in clear bottom 96-well plates (ViewPlate 96, Perkin Elmer), were washed with ice-cold PBS and fixed with 100µl/well of 4% PFA. After washing with PBS and blocking with PBS containing 5% nonfat dry milk and 5% BSA, the samples were incubated with primary anti-TRKB antibody (R&D Systems, #AF1494, 1:1000 in blocking buffer) ON at 4ºC. Following washing, the samples were incubated with HRP-conjugated anti goat IgG (1:5000 in blocking buffer) for 1h at RT. The cells were washed 4x with 200µl of PBS for 10 min each. Finally, the chemiluminescent signal generated by reaction with ECL was analyzed in a plate reader.
The levels of total and phosphorylated TRKB at Y515 or Y816 in MG87.TRKB cells, challenged with BDNF, were measured by western-blotting (Rantamäki et al., 2007).
For the analysis of TRKB migration to lipid rafts, the samples from transfected N2A cells to express GFP-tagged TRKB.wt or TRKB.Y433F, challenged with BDNF, were processed to isolate detergent-resistant membrane (DRM) fractions in sucrose gradient (McGuinn and Mahoney, 2014). N2A cells were seeded at a density of 2.5 million per plate on 10 cm plates and transfected after 24 hours with either wild-type GFP-tagged full length TRKB or the GFP-tagged Y433F TRKB mutant. 48 hours after plating, cells were washed with ice cold 1x PBS and scraped in extraction buffer (25 mM Tris-HCl pH 8, 150 mM NaCl, 5 mM EDTA) with the addition of 0.5% v/v Lubrol (Serva) and a cocktail of protease and phosphatase inhibitors (Sigma). Cellular membranes were mechanically broken by passing the cell suspension through a 23G needle five times. Protein concentration was measured for each sample and equal amounts of proteins were transferred to Eppendorf tubes and mixed with sucrose in the extraction buffer to a final concentration of 72% . The samples were then transferred to the bottom of Beckman 2.2 ml ultracentrifuge tubes and carefully covered with equal volumes of 35% sucrose and 5% sucrose in extraction buffer.

The samples were centrifuged at 52000 x g for 18 hours at +4°C with a TLS-55 rotor in a Beckman Coulter XP Optima ultracentrifuge. Finally, 12 fractions per sample, collected from the top of the tube, were transferred to clean tubes, sonicated for 10 minutes in 0.25% SDS and prepared for western blotting, where the levels of GFP-tagged TRKB and flotillin-2 were analyzed.

Protein complementation assay: two complementary fragments of the luciferase reporter protein were fused to the intracellular C-terminus domain of TRKB.wt or mutant TRKB.Y433F to produce the PCA pairs GLuc1C-TRKB.wt/GLuc2C-TRKB.wt and GLuc1C-TRKB.Y433F/GLuc2C-TRKB.Y433F. Alternatively, the GLuc1C-TRKB.wt/GLuc2C-FYN or GLuc1C-TRKB.Y433F/GLuc2C-FYN pairs were used. The GLuc2C-FYN construct expresses a lipid-raft restricted fragment of Src-family kinase FYN (Merezhko et al., 2020). The GLuc tag was linked via a GS linker that allows the physiological dynamics of proteins without interferences from the presence of the tag. N2A cells, in 10% (v/v) poly-L-Lysine coated 96 wells (10,000 cells/well) were transfected with the construct pairs above. Cells were treated 48h post-transfection with BDNF (10ng/ml/10min), and luminescence measured as a direct indication of TRKB homodimerization or TRKB:LR-FYN with a plate reader (Varioskan Flash, Thermo Scientific, average of 5 measurements, 0.1 second each) immediately after the injection of the coelenterazine substrate (Nanolight Technology).

Cell viability: the assay was performed using CellTiterGlo (#G7571; Promega) according to the manufacturer's instructions. Briefly, equal amounts of medium and the mixture of regents A and B were added to the E18 cortical cells (DIV8) and incubated for 40min in clear bottom 96-well plates. . The cells were previously treated with BDNF (10ng/ml/5d), cholesterol (20µM/5d) or combo and pravastatin (2µM/5d). The luminescence was analyzed in a plate reader.

Drug binding assay: the drug/BDNF interaction with TRKB was determined by ELISA, based on similar assays in literature (Das et al., 2015). TRKB.wt or TRKB.Y433F were expressed in HEK293T cells, and immunoprecipitated in 96-well plates. Increasing doses of biotinylated drugs fluoxetine or R,R-HNK (0.1-100µM), tritiated imipramine (0.01-30µM) or biotinylated BDNF (0.1-100ng/ml) were added after blocking with 2% BSA in PBS for 1h and the signal developed by incubation with HRP-conjugated streptavidin followed by ECL. For the competitive assay, increased doses of non-biotinylated drugs (0.1-10µM) or BDNF (10-100ng/ml) were mixed with 1µM of biotinylated fluoxetine for 1h, and the signal from HRP-conjugated streptavidin developed as described above. Microscale Thermophoresis - MST - was performed according to literature (Jerabek-Willemsen et al., 2014). Briefly, the changes in fluorescence following temperature gradient emitted by GFP-TRKB, incubated with fluoxetine (0-100µM) were conducted in premium coated capillaries using LED source with 470nm and 50% infrared-laser power.

FRAP: hippocampal cells from E18 rat embryos (DIV14) were transfected to express GFP-TRKB.wt or GFP-TRKB.Y433F. Upon identification of GFP-positive cells, the cells were treated with fluoxetine, ketamine or BDNF for 15min; the whole spine head or the neurite shaft was bleached with high laser power (Koskinen et al., 2012) and the latency for fluorescence recovery was quantified.

TIRF/dSTORM: MG87.TRKB cells were transfected to overexpress GFP-TRKB.wt or GFP-TRKB.Y433F, challenged with BDNFor fluoxetine for 15min and fixed to immunostaining for GFP. The area of GFP-tagged TRKB cell surface clusters was determined by total internal reflection fluorescence microscopy (TIRF) coupled with direct stochastic optical reconstruction microscopy (dSTORM).

Immunostaining and Sholl analysis: cortical cells (E18 rat embryo, DIV8) were treated with BDNF (10ng/ml/3d) and pravastatin (1µM/3d), fixed and labeled for actin. The number of intersections from the cell body was counted using FIJI plug-in (Schindelin et al., 2012).

Electrophysiology (details in supplement): in vivo and ex vivo:

In vivo BDNF-induced LTP was performed according to literature (Panja and Bramham, 2014). Briefly, pravastatin was administered in drinking water at a dose of 10mg/kg/day for 15-17 days calculated on the basis of daily body weight. Rats were anesthetized with an intraperitoneal injection of urethane 1.5 g/kg body weight, positioned in a stereotaxic frame, and Teflon-coated tungsten wire recording electrode was placed in the dentate hilus. The tip of the infusion cannula was located in the deep stratum lacunosum-moleculare of field CA1, 800µm above the hilar recording site and 300-400µm above the medial perforant synapse. After baseline recording for 20 min, infusion of 2µl of 1 µg/µl BDNF over 30 min at a rate of 0.067µl/min. Evoked responses were recorded for 120 min after infusion.
Ex vivo activity-induced LTP: TBS and tetanus stimulus was performed according to literature (Popova et al., 2017). Briefly, mice were deeply anaesthetized with isoflurane, the brains were dissected and horizontal 350 micrometers brain slices of the hippocampus were cut on a vibratome. Field excitatory postsynaptic currents (EPSPs) were recorded at the stratum radiatum of the CA1 region. Electric stimulation was delivered by a bipolar concentric stimulation electrode placed at the Schaffer collateral. After obtaining a 15 min stable baseline theta burst stimulation (TBS: 10 bursts of four pulses at 100 Hz, with an interburst interval of 200 msec) or tetanic stimulation (200ms pulse interval; 100 pulses; 0.1ms pulse duration) was delivered and field potentials were recorded for 45 min.

Ocular dominance plasticity assay (details in supplement):
The shift in ocular dominance induced by drug treatment was performed according to literature (Steinzeig et al., 2017). Briefly, animals were anesthetized via i.p. injection with a mixture containing: 0.05 mg/kg fentanyl; 5 mg/kg midazolam; 0.5 mg/kg medetomidine; diluted in saline and fixed in the stereotaxic frame. After cleaning and polishing, a thin layer of cyanoacrylate glue was applied to the surface of the skull, in order to make it transparent. The next day, the acryl layer was polished over the area of interest. A metal head holder was first glued on the skull, carefully keeping the area of interest at the center of the holder, and then fixed with a mixture of cyanoacrylate glue and dental cement. Finally, transparent nail polisher (#72180, Electron Microscopy Sciences) was applied inside the metal holder above the area of interest. Monocular deprivation was carried on the left eye, the eyelashes were cut and the eye sutured shut with 3 mattress sutures. The monocular deprivation lasted 8 days and the animals were checked daily and resutured if needed to prevent reopening of the eyes. Two sessions of imaging were performed: one before the beginning of the treatment with fluoxetine, ketamine or R,R-HNK (IOS I) and one on the 8th day after monocular deprivation (IOS II). For imaging, animals were kept on a heating pad located in front of and within 25 cm from the stimulus monitor. The visual stimulus was a 2° wide horizontal bar moving upwards with a temporal frequency of 0.125 Hz and a spatial frequency of 1/80 degree, displayed in the central part of a high refresh rate monitor (-15 to 5 degrees azimuth, relative to the animal visual field) in order to preferentially stimulate the binocular part of the visual field. The continuous-periodic stimulation was synchronized with a continuous frame acquisition, frames were collected independently for each eye. After obtaining cortical maps for both contralateral (C) and ipsilateral (I) eyes and computing Ocular Dominance score as $(C-I)/(C+I)$, finally, the Optical Dominance Index (ODI) was calculated as the mean of the OD score for all responsive pixels. The ODI values are comprised in an interval going from -1 to +1: positive values indicate a contralateral bias, negative ones indicate ipsilateral bias and ODI values of 0 indicate that ipsilateral and contralateral eyes are equally strong.

Behavioral analysis:
Object-location memory (OLM): this test was performed in a square arena (28cm side) with opaque walls containing cues (black stripes or spots). The mice were placed for 3 consecutive days (15min per session) in the arena with two identical objects (table tennis balls glued to caps of 50ml Falcon tubes) in the same position throughout the sessions (pretest). Following the drug administration (starting immediately after the last pretest session). At the test session one of the objects is moved to a different position and the number of visits (counted as sniffing or interacting with the object) to the old (A) or newly located (A') object was determined by an observer blind to the conditions (Ampuero et al., 2013; Dere et al., 2007).
Contextual fear conditioning: this test was modified from previous studies (Karpova et al., 2011). Briefly,

the mice were conditioned to 5 scrambled foot shocks (0.6mA/2s) during the 8 min session (arena: 23×23×35cm) under constant illumination (100 lux). The treatment with fluoxetine started immediately after the conditioning session throughout the last extinction trial. During the extinction trials, the animals were exposed to the same context where the shocks were delivered and the time spent in freezing during the 8 min session was automatically determined by the software (TSE Systems, Germany).
Forced swimming test - FST: animals were submitted to a 6min session of FST in 5-liter glass beaker cylinders (19cm diameter, with 20cm water column 25±1ºC) (Diniz et al., 2018). Fluoxetine was administered for 3weeks (15mg/kg, in the drinking water), and ketamine was injected 2h (ip) prior to the FST. The immobility was assessed in the last 4min of the session, and the water was changed between each test. After swimming, animals were kept in a warm cage until dried, then returned to their home cages. Test was videotaped and analyzed by a trained observer blind to treatment.

Statistics: Student's t test (two-tailed), one- or two-way ANOVA were used, followed by Fisher's LSD *post hoc* test. *F* and *p* values are indicated in figure legends.

References

Abdallah, C.G., Sanacora, G., Duman, R.S., and Krystal, J.H. (2015). Ketamine and rapid-acting antidepressants: a window into a new neurobiology for mood disorder therapeutics. Annu. Rev. Med. *66*, 509–523.

Abraham, M.J., Murtola, T., Schulz, R., Páll, S., Smith, J.C., Hess, B., and Lindahl, E. (2015). GROMACS: High performance molecular simulations through multi-level parallelism from laptops to supercomputers. SoftwareX *1-2*, 19–25.

Alford, R.F., Koehler Leman, J., Weitzner, B.D., Duran, A.M., Tilley, D.C., Elazar, A., and Gray, J.J. (2015). An Integrated Framework Advancing Membrane Protein Modeling and Design. PLoS Comput. Biol. *11*, e1004398.

Ampuero, E., Stehberg, J., Gonzalez, D., Besser, N., Ferrero, M., Diaz-Veliz, G., Wyneken, U., and Rubio, F.J. (2013). Repetitive fluoxetine treatment affects long-term memories but not learning. Behav. Brain Res. *247*, 92–100.

Andero, R., and Ressler, K.J. (2012). Fear extinction and BDNF: translating animal models of PTSD to the clinic. Genes Brain Behav. *11*, 503–512.

Antila, H., Autio, H., Turunen, L., Harju, K., Tammela, P., Wennerberg, K., Yli-Kauhaluoma, J., Huttunen, H.J., Castrén, E., and Rantamäki, T. (2014). Utilization of in situ ELISA method for examining Trk receptor phosphorylation in cultured cells. J. Neurosci. Methods *222*, 142–146.

Arkhipov, A., Shan, Y., Das, R., Endres, N.F., Eastwood, M.P., Wemmer, D.E., Kuriyan, J., and Shaw, D.E. (2013). Architecture and membrane interactions of the EGF receptor. Cell *152*, 557–569.

Autry, A.E., and Monteggia, L.M. (2012). Brain-derived neurotrophic factor and neuropsychiatric disorders. Pharmacol. Rev. *64*, 238–258.

Beglov, D., and Roux, B. (1994). Finite representation of an infinite bulk system: Solvent boundary potential for computer simulations. J. Chem. Phys. *100*, 9050–9063.

Belmaker, R.H., and Agam, G. (2008). Major depressive disorder. N. Engl. J. Med. *358*, 55–68.

Berman, R.M., Cappiello, A., Anand, A., Oren, D.A., Heninger, G.R., Charney, D.S., and Krystal, J.H. (2000). Antidepressant effects of ketamine in depressed patients. Biol. Psychiatry *47*, 351–354.

Bolo, N.R., Hodé, Y., Nédélec, J.F., Lainé, E., Wagner, G., and Macher, J.P. (2000). Brain pharmacokinetics and tissue distribution in vivo of fluvoxamine and fluoxetine by fluorine magnetic resonance spectroscopy. Neuropsychopharmacology *23*, 428–438.

Cang, J., Kalatsky, V.A., Löwel, S., and Stryker, M.P. (2005). Optical imaging of the intrinsic signal as a measure of cortical plasticity in the mouse. Vis. Neurosci. *22*, 685–691.

Castrén, E., and Antila, H. (2017). Neuronal plasticity and neurotrophic factors in drug responses. Mol. Psychiatry.

Chen, J., Korostyshevsky, D., Lee, S., and Perlstein, E.O. (2012). Accumulation of an antidepressant in vesiculogenic membranes of yeast cells triggers autophagy. PLoS One *7*, e34024.

Das, I., Krzyzosiak, A., Schneider, K., Wrabetz, L., D'Antonio, M., Barry, N., Sigurdardottir, A., and Bertolotti, A. (2015). Preventing proteostasis diseases by selective inhibition of a phosphatase regulatory subunit. Science *348*, 239–242.

Dekkers, M.P.J., Nikoletopoulou, V., and Barde, Y.-A. (2013). Cell biology in neuroscience: Death of developing neurons: new insights and implications for connectivity. J. Cell Biol. *203*, 385–393.

Dere, E., Huston, J.P., and De Souza Silva, M.A. (2007). The pharmacology, neuroanatomy and neurogenetics of one-trial object recognition in rodents. Neurosci. Biobehav. Rev. *31*, 673–704.

Deschaux, O., Spennato, G., Moreau, J.-L., and Garcia, R. (2011). Chronic treatment with fluoxetine prevents the return of extinguished auditory-cued conditioned fear. Psychopharmacology *215*, 231–237.

Di Lieto, A., Rantamäki, T., Vesa, L., Yanpallewar, S., Antila, H., Lindholm, J., Rios, M., Tessarollo, L., and Castrén, E. (2012). The responsiveness of TrkB to BDNF and antidepressant drugs is differentially regulated during mouse development. PLoS One *7*, e32869.

Diniz, C.R.A.F., Casarotto, P.C., Fred, S.M., Biojone, C., Castrén, E., and Joca, S.R.L. (2018). Antidepressant-like effect of losartan involves TRKB transactivation from angiotensin receptor type 2 (AGTR2) and recruitment of FYN. Neuropharmacology *135*, 163–171.

Du, J., Feng, L., Yang, F., and Lu, B. (2000). Activity- and Ca(2+)-dependent modulation of surface expression of brain-derived neurotrophic factor receptors in hippocampal neurons. J. Cell Biol. *150*, 1423–1434.

Duman, R.S., and Monteggia, L.M. (2006). A neurotrophic model for stress-related mood disorders. Biol. Psychiatry *59*, 1116–1127.

Endres, N.F., Das, R., Smith, A.W., Arkhipov, A., Kovacs, E., Huang, Y., Pelton, J.G., Shan, Y., Shaw, D.E., Wemmer, D.E., et al. (2013). Conformational coupling across the plasma membrane in activation of the EGF receptor. Cell *152*, 543–556.

Erb, S.J., Schappi, J.M., and Rasenick, M.M. (2016). Antidepressants Accumulate in Lipid Rafts Independent of Monoamine Transporters to Modulate Redistribution of the G Protein, Gαs. J. Biol. Chem. *291*, 19725–19733.

Ernfors, P., and Bramham, C.R. (2003). The coupling of a trkB tyrosine residue to LTP. Trends Neurosci. *26*, 171–173.

Fantini, J., and Barrantes, F.J. (2013). How cholesterol interacts with membrane proteins: an exploration of cholesterol-binding sites including CRAC, CARC, and tilted domains. Front. Physiol. *4*.

Fantini, J., Epand, R.M., and Barrantes, F.J. (2019). Cholesterol-Recognition Motifs in Membrane Proteins. Adv. Exp. Med. Biol. *1135*, 3–25.

Fleishman, S.J., Leaver-Fay, A., Corn, J.E., Strauch, E.-M., Khare, S.D., Koga, N., Ashworth, J., Murphy, P., Richter, F., Lemmon, G., et al. (2011). RosettaScripts: a scripting language interface to the Rosetta macromolecular modeling suite. PLoS One *6*, e20161.

Fred, S.M., Laukkanen, L., Brunello, C.A., Vesa, L., Göös, H., Cardon, I., Moliner, R., Maritzen, T., Varjosalo, M., Casarotto, P.C., et al. (2019). Pharmacologically diverse antidepressants facilitate TRKB receptor activation by disrupting its interaction with the endocytic adaptor complex AP-2. J. Biol. Chem.

Greifzu, F., Schmidt, S., Schmidt, K.-F., Kreikemeier, K., Witte, O.W., and Löwel, S. (2011). Global impairment and therapeutic restoration of visual plasticity mechanisms after a localized cortical stroke. Proc. Natl. Acad. Sci. U. S. A. *108*, 15450–15455.

Haapasalo, A., Sipola, I., Larsson, K., Akerman, K.E.O., Stoilov, P., Stamm, S., Wong, G., and Castren, E. (2002). Regulation of TRKB surface expression by brain-derived neurotrophic factor and truncated TRKB isoforms. J. Biol. Chem. *277*, 43160–43167.

Henry, M.E., Moore, C.M., Kaufman, M.J., Michelson, D., Schmidt, M.E., Stoddard, E., Vuckevic, A.J., Berreira, P.J., Cohen, B.M., and Renshaw, P.F. (2000). Brain kinetics of paroxetine and fluoxetine on the third day of placebo substitution: a fluorine MRS study. Am. J. Psychiatry *157*, 1506–1508.

Huang, J., Rauscher, S., Nawrocki, G., Ran, T., Feig, M., Groot, B.L. de, Grubmüller, H., and Jr, A.D.M. (2017). CHARMM36m: an improved force field for folded and intrinsically disordered proteins. Nat. Methods *14*, 71–73.

Humphrey, W., Dalke, A., and Schulten, K. (1996). VMD: visual molecular dynamics. J. Mol. Graph. *14*, 33–38, 27–28.

Ikonen, E. (2008). Cellular cholesterol trafficking and compartmentalization. Nat. Rev. Mol. Cell Biol. *9*, 125–138.

Jerabek-Willemsen, M., André, T., Wanner, R., Roth, H.M., Duhr, S., Baaske, P., and Breitsprecher, D. (2014). MicroScale Thermophoresis: Interaction analysis and beyond. J. Mol. Struct. *1077*, 101–113.

Jo, S., Kim, T., Iyer, V.G., and Im, W. (2008). CHARMM-GUI: a web-based graphical user interface for CHARMM. J. Comput. Chem. *29*, 1859–1865.

Jorgensen, W.L., Chandrasekhar, J., Madura, J.D., Impey, R.W., and Klein, M.L. (1983). Comparison of simple potential functions for simulating liquid water. J. Chem. Phys. *79*, 926–935.

Kang, H., Welcher, A.A., Shelton, D., and Schuman, E.M. (1997). Neurotrophins and time: different roles for TrkB signaling in hippocampal long-term potentiation. Neuron *19*, 653–664.

Karpova, N.N., Pickenhagen, A., Lindholm, J., Tiraboschi, E., Kulesskaya, N., Agústsdóttir, A., Antila, H., Popova, D., Akamine, Y., Bahi, A., et al. (2011). Fear erasure in mice requires synergy between antidepressant drugs and extinction training. Science *334*, 1731–1734.

Karson, C.N., Newton, J.E., Livingston, R., Jolly, J.B., Cooper, T.B., Sprigg, J., and Komoroski, R.A. (1993). Human brain fluoxetine concentrations. J. Neuropsychiatry Clin. Neurosci. *5*, 322–329.

Klauda, J.B., Venable, R.M., Freites, J.A., O'Connor, J.W., Tobias, D.J., Mondragon-Ramirez, C., Vorobyov, I., MacKerell, A.D., and Pastor, R.W. (2010). Update of the CHARMM all-atom additive force field for lipids: validation on six lipid types. J. Phys. Chem. B *114*, 7830–7843.

Klimovich, P.V., Shirts, M.R., and Mobley, D.L. (2015). Guidelines for the analysis of free energy calculations. J. Comput. Aided Mol. Des. *29*, 397–411.

Koponen, E., Rantamäki, T., Voikar, V., Saarelainen, T., MacDonald, E., and Castrén, E. (2005). Enhanced BDNF signaling is associated with an antidepressant-like behavioral response and changes in brain monoamines. Cell. Mol. Neurobiol. *25*, 973–980.

Kornhuber, J., Retz, W., and Riederer, P. (1995). Slow accumulation of psychotropic substances in the human brain. Relationship to therapeutic latency of neuroleptic and antidepressant drugs? J. Neural Transm. Suppl. *46*, 315–323.

Koskinen, M., Bertling, E., and Hotulainen, P. (2012). Methods to measure actin treadmilling rate in dendritic spines. Methods Enzymol. *505*, 47–58.

Li, E., Wimley, W.C., and Hristova, K. (2012). Transmembrane helix dimerization: beyond the search for sequence motifs. Biochim. Biophys. Acta *1818*, 183–193.

Lindholm, J.S.O., and Castrén, E. (2014). Mice with altered BDNF signaling as models for mood disorders and antidepressant effects. Front. Behav. Neurosci. *8*, 143.

Lomize, A.L., Hage, J.M., and Pogozheva, I.D. (2018). Membranome 2.0: database for proteome-wide profiling of bitopic proteins and their dimers. Bioinformatics *34*, 1061–1062.

Martin, M.G., Ahmed, T., Korovaichuk, A., Venero, C., Menchón, S.A., Salas, I., Munck, S., Herreras, O., Balschun, D., and Dotti, C.G. (2014). Constitutive hippocampal cholesterol loss underlies poor cognition in old rodents. EMBO Mol. Med. *6*, 902–917.

Mauch, D.H., Nägler, K., Schumacher, S., Göritz, C., Müller, E.C., Otto, A., and Pfrieger, F.W. (2001). CNS Synaptogenesis Promoted by Glia-Derived Cholesterol. Science *294*, 1354–1357.

Maya Vetencourt, J.F., Sale, A., Viegi, A., Baroncelli, L., De Pasquale, R., O'Leary, O.F., Castrén, E., and Maffei, L. (2008). The antidepressant fluoxetine restores plasticity in the adult visual cortex. Science *320*, 385–388.

McGuinn, K.P., and Mahoney, M.G. (2014). Lipid rafts and detergent-resistant membranes in epithelial keratinocytes. Methods Mol. Biol. *1195*, 133–144.

Merezhko, M., Pakarinen, E., Uronen, R.-L., and Huttunen, H.J. (2020). Live-cell monitoring of protein localization to membrane rafts using protein-fragment complementation. Biosci. Rep. *40*.

Messaoudi, E., Ying, S.-W., Kanhema, T., Croll, S.D., and Bramham, C.R. (2002). Brain-derived neurotrophic factor triggers transcription-dependent, late phase long-term potentiation in vivo. J. Neurosci. *22*, 7453–7461.

Meyer-Franke, A., Wilkinson, G.A., Kruttgen, A., Hu, M., Munro, E., Hanson, M.G., Jr, Reichardt, L.F., and Barres, B.A. (1998). Depolarization and cAMP elevation rapidly recruit TrkB to the plasma membrane of CNS neurons. Neuron *21*, 681–693.

Minichiello, L. (2009). TrkB signalling pathways in LTP and learning. Nat. Rev. Neurosci. *10*, 850–860.

Minichiello, L., Calella, A.M., Medina, D.L., Bonhoeffer, T., Klein, R., and Korte, M. (2002). Mechanism of TrkB-mediated hippocampal long-term potentiation. Neuron *36*, 121–137.

Monteggia, L.M., Barrot, M., Powell, C.M., Berton, O., Galanis, V., Gemelli, T., Meuth, S., Nagy, A., Greene, R.W., and Nestler, E.J. (2004). Essential role of brain-derived neurotrophic factor in adult hippocampal function. Proc. Natl. Acad. Sci. U. S. A. *101*, 10827–10832.

Nackenoff, A.G., Moussa-Tooks, A.B., McMeekin, A.M., Veenstra-VanderWeele, J., and Blakely, R.D. (2016). Essential Contributions of Serotonin Transporter Inhibition to the Acute and Chronic Actions of Fluoxetine and Citalopram in the SERT Met172 Mouse. Neuropsychopharmacology *41*, 1733–1741.

Nikoletopoulou, V., Lickert, H., Frade, J.M., Rencurel, C., Giallonardo, P., Zhang, L., Bibel, M., and Barde, Y.-A. (2010). Neurotrophin receptors TrkA and TrkC cause neuronal death whereas TrkB does not. Nature *467*, 59–63.

Normann, C., Frase, S., Haug, V., von Wolff, G., Clark, K., Münzer, P., Dorner, A., Scholliers, J., Horn, M., Vo Van, T., et al. (2018). Antidepressants Rescue Stress-Induced Disruption of Synaptic Plasticity via Serotonin Transporter-Independent Inhibition of L-Type Calcium Channels. Biol. Psychiatry *84*, 55–64.

Pampallona, S., Bollini, P., Tibaldi, G., Kupelnick, B., and Munizza, C. (2004). Combined pharmacotherapy and psychological treatment for depression: a systematic review. Arch. Gen. Psychiatry *61*, 714–719.

Panja, D., and Bramham, C.R. (2014). BDNF mechanisms in late LTP formation: A synthesis and breakdown. Neuropharmacology *76 Pt C*, 664–676.

Park, H., and Poo, M.-M. (2013). Neurotrophin regulation of neural circuit development and function. Nat. Rev. Neurosci. *14*, 7–23.

Patterson, S.L., Pittenger, C., Morozov, A., Martin, K.C., Scanlin, H., Drake, C., and Kandel, E.R. (2001). Some forms of cAMP-mediated long-lasting potentiation are associated with release of BDNF and nuclear translocation of phospho-MAP kinase. Neuron *32*, 123–140.

Pereira, D.B., and Chao, M.V. (2007). The tyrosine kinase Fyn determines the localization of TrkB receptors in lipid rafts. J.

Neurosci. *27*, 4859–4869.

Pfrieger, F.W., and Ungerer, N. (2011). Cholesterol metabolism in neurons and astrocytes. Prog. Lipid Res. *50*, 357–371.

Popova, D., Castrén, E., and Taira, T. (2017). Chronic fluoxetine administration enhances synaptic plasticity and increases functional dynamics in hippocampal CA3-CA1 synapses. Neuropharmacology *126*, 250–256.

Rantamäki, T., Hendolin, P., Kankaanpää, A., Mijatovic, J., Piepponen, P., Domenici, E., Chao, M.V., Männistö, P.T., and Castrén, E. (2007). Pharmacologically diverse antidepressants rapidly activate brain-derived neurotrophic factor receptor TrkB and induce phospholipase-Cgamma signaling pathways in mouse brain. Neuropsychopharmacology *32*, 2152–2162.

Saarelainen, T., Hendolin, P., Lucas, G., Koponen, E., Sairanen, M., MacDonald, E., Agerman, K., Haapasalo, A., Nawa, H., Aloyz, R., et al. (2003). Activation of the TrkB neurotrophin receptor is induced by antidepressant drugs and is required for antidepressant-induced behavioral effects. J. Neurosci. *23*, 349–357.

Sahu, M.P., Nikkilä, O., Lågas, S., Kolehmainen, S., and Castrén, E. (2019). Culturing primary neurons from rat hippocampus and cortex. Neuronal Signaling *3*, NS20180207.

Schindelin, J., Arganda-Carreras, I., Frise, E., Kaynig, V., Longair, M., Pietzsch, T., Preibisch, S., Rueden, C., Saalfeld, S., Schmid, B., et al. (2012). Fiji: an open-source platform for biological-image analysis. Nat. Methods *9*, 676–682.

Senes, A., Engel, D.E., and DeGrado, W.F. (2004). Folding of helical membrane proteins: the role of polar, GxxxG-like and proline motifs. Curr. Opin. Struct. Biol. *14*, 465–479.

Sinclair, J.K.L., Walker, A.S., Doerner, A.E., and Schepartz, A. (2018). Mechanism of Allosteric Coupling into and through the Plasma Membrane by EGFR. Cell Chem Biol *25*, 857–870.e7.

Steinzeig, A., Molotkov, D., and Castrén, E. (2017). Chronic imaging through “transparent skull” in mice. PLoS One *12*, e0181788.

Suzuki, S., Numakawa, T., Shimazu, K., Koshimizu, H., Hara, T., Hatanaka, H., Mei, L., Lu, B., and Kojima, M. (2004). BDNF-induced recruitment of TrkB receptor into neuronal lipid rafts: roles in synaptic modulation. J. Cell Biol. *167*, 1205–1215.

Suzuki, S., Kiyosue, K., Hazama, S., Ogura, A., Kashihara, M., Hara, T., Koshimizu, H., and Kojima, M. (2007). Brain-Derived Neurotrophic Factor Regulates Cholesterol Metabolism for Synapse Development. Journal of Neuroscience *27*, 6417–6427.

Tulodziecka, K., Diaz-Rohrer, B.B., Farley, M.M., Chan, R.B., Di Paolo, G., Levental, K.R., Waxham, M.N., and Levental, I. (2016). Remodeling of the postsynaptic plasma membrane during neural development. Mol. Biol. Cell *27*, 3480–3489.

Vanommeslaeghe, K., Hatcher, E., Acharya, C., Kundu, S., Zhong, S., Shim, J., Darian, E., Guvench, O., Lopes, P., Vorobyov, I., et al. (2009). CHARMM general force field: A force field for drug-like molecules compatible with the CHARMM all-atom additive biological force fields. J. Comput. Chem. *31*, 671–690.

Wiesel, T.N. (1982). Postnatal development of the visual cortex and the influence of environment. Nature *299*, 583–591.

Wray, N.H., Schappi, J.M., Singh, H., Senese, N.B., and Rasenick, M.M. (2018). NMDAR-independent, cAMP-dependent antidepressant actions of ketamine. Mol. Psychiatry.

Xia, Z., Dudek, H., Miranti, C.K., and Greenberg, M.E. (1996). Calcium influx via the NMDA receptor induces immediate early gene transcription by a MAP kinase/ERK-dependent mechanism. J. Neurosci. *16*, 5425–5436.

Zanos, P., Moaddel, R., Morris, P.J., Georgiou, P., Fischell, J., Elmer, G.I., Alkondon, M., Yuan, P., Pribut, H.J., Singh, N.S., et al. (2016). NMDAR inhibition-independent antidepressant actions of ketamine metabolites. Nature *533*, 481–486.

Zanos, P., Moaddel, R., Morris, P.J., Riggs, L.M., Highland, J.N., Georgiou, P., Pereira, E.F.R., Albuquerque, E.X., Thomas, C.J., Zarate, C.A., Jr, et al. (2018). Ketamine and Ketamine Metabolite Pharmacology: Insights into Therapeutic Mechanisms. Pharmacol. Rev. *70*, 621–660.

Zarate, C.A., Jr, Singh, J.B., Carlson, P.J., Brutsche, N.E., Ameli, R., Luckenbaugh, D.A., Charney, D.S., and Manji, H.K. (2006). A randomized trial of an N-methyl-D-aspartate antagonist in treatment-resistant major depression. Arch. Gen. Psychiatry *63*, 856–864.

Zonta, B., and Minichiello, L. (2013). Synaptic membrane rafts: traffic lights for local neurotrophin signaling? Front. Synaptic Neurosci. *5*.